HHS Public Access

Author manuscript

Biomaterials. Author manuscript; available in PMC 2017 January 01.

Published in final edited form as:

Biomaterials. 2016 January ; 75: 193–202. doi:10.1016/j.biomaterials.2015.10.027.

Doxorubicin Encapsulated in Stealth Liposomes Conferred with Light-Triggered Drug Release

Dandan Luo[1], **Kevin A Carter**[1], **Aida Razi**[2], **Jumin Geng**[1], **Shuai Shao**[1], **Daniel Giraldo**[1], **Ulas Sunar**[3], **Joaquin Ortega**[2], and **Jonathan F. Lovell**[1,*]

[1]Department of Biomedical Engineering, University at Buffalo, State University of New York, Buffalo, NY, 14260

[2]Department of Biochemistry and Biomedical Sciences and M. G. DeGroote Institute for Infectious Diseases Research, McMaster University, Hamilton, ON, L8S4L8

[3]Department of Biomedical, Industrial & Human Factors Engineering, Wright State University, Dayton, OH, 45435

Abstract

Stealth liposomes can be used to extend the blood circulation time of encapsulated therapeutics. Inclusion of 2 molar % porphyrin-phospholipid (PoP) imparted optimal near infrared (NIR) light-triggered release of doxorubicin (Dox) from conventional sterically stabilized stealth liposomes. The type and amount of PoP affected drug loading, serum stability and drug release induced by NIR light. Cholesterol and PEGylation were required for Dox loading, but slowed light-triggered release. Dox in stealth PoP liposomes had a long circulation half-life in mice of 21.9 hours and was stable in storage for months. Following intravenous injection and NIR irradiation, Dox deposition increased ~7 fold in treated subcutaneous human pancreatic xenografts. Phototreatment induced mild tumor heating and complex tumor hemodynamics. A single chemophototherapy treatment with Dox-loaded stealth PoP liposomes (at 5–7 mg/kg Dox) eradicated tumors while corresponding chemo- or photodynamic therapies were ineffective. A low dose 3 mg/kg Dox phototreatment with stealth PoP liposomes was more effective than a maximum tolerated dose of free (7 mg/kg) or conventional long-circulating liposomal Dox (21 mg/kg). To our knowledge, Dox-loaded stealth PoP liposomes represent the first reported long-circulating nanoparticle capable of light-triggered drug release.

Keywords

Liposomes; Chemotherapy; Phototherapy; Doxorubicin; Porphyrin-phospholipid; Chemophototherapy

Contact: jflovell@buffalo.edu.

Preferential accumulation of drugs at target sites in bioavailable form is a central goal of drug delivery systems.[1–4] Liposomes are applied for this purpose and are commonly used pharmaceutical carriers.[5,6] By incorporating a synthetic polyethylene glycol phospholipid (DSPE-PEG-2K) into stable liposomes, sterically stabilized "stealth" liposomes are obtained and can substantially prolong drug circulating time and increase drug accumulation in the tumors with enhanced antitumor efficacy.[7–10] However, once localized in the tumor, the drug should be released at an appropriate rate to ensure therapeutic concentrations reach target cells. Long circulating stealth liposomes release their cargo slowly, which limits efficacy in cancer treatment[11,12]. Exposure of large amounts of bioavailable drug in tumors is desirable, while ideally reducing exposure to healthy organs.[1,13,14]. Remotely-triggered drug delivery systems hold potential to meet this need.[15,16] There has been interest in developing liposomes that effectively encapsulate anti-cancer agents and release them specifically within tumors. To this end, many liposome triggered-release strategies have been developed including activation methods based on pH [17–20], heat [13,21,22], enzymes[23,24], light[3,25,26] and magnetic pulses[27] and thermosensitive liposomes have entered clinical testing for multiple cancer indications.[28]

Light, especially near infrared (NIR) light which can better penetrate tissues and is otherwise harmless itself, is an intriguing external trigger for drug release and can be applied with precise spatial and temporal control.[3,26,29,30] There has been much recent interest in development of light-triggered drug delivery systems.[31–39] Compared to thermosensitive liposomes, which have been extensively studied for more than three decades[40,41], light triggered release has seen less development and the release mechanisms, factors controlling the release rate and design strategies are still emerging. However, thermosensitive liposomes and other heat-triggered mechanisms (including photothermally triggered) generally have limited stability in physiological conditions due to difficulty in developing materials that are stable at 37 °C but that can release their contents close to 42 °C. There have been only a few reports of long-circulating thermosensitive materials, and drugs loaded into such carriers only have a fraction of the circulation time of conventional stealth liposomes.[42] To our knowledge, until now there have not yet been any reports of long-circulating nanoparticles for light-triggered release.

Porphyrin-phospholipid (PoP) is a lipid-like molecule and can be used to form nanoparticles with theranostic character.[43–48] The structure of the PoPs used in this study comprise a monocarboxylic porphyrin derivative esterified to the central sn-2 hydroxyl of the glycerol backbone of phosphatidylcholine containing a palmitoyl group at the sn-1 position. The chlorophyll derived pyropheophorbide-*a* (Pyro) or related 2-[1-hexyloxyethyl]-2-devinyl pyropheophorbide-*a* (HPPH) were used to generate Pyro-lipid or HPPH-lipid respectively. We previously reported that PoP-liposomes based on HPPH-lipid can release their contents in response to NIR light, via a mechanism that is still unknown.[26] However, relatively high amounts of HPPH-lipid were required, which in theory could lead to patient side effects such as sunlight-induced or treatment-induced cutaneous toxicity.[49–51] Furthermore, examination of HPPH-lipid liposomes revealed that the stability in 50 % serum was poor and light-triggered release rates were less than ideal. Here, we describe a systematic

approach to develop stealth PoP liposomes with balanced lipid ratios to achieve both rapid light release rate and high storage and serum stability with long blood circulation.

Materials and Methods

Preparation of PoP liposomes

Unless otherwise noted, lipids were obtained from Avanti and other materials were obtained from Sigma. HPPH-lipid and Pyro-lipid were synthesized as previously reported.[26] Various liposome formulations were all made using the same method. The finalized stealth PoP liposome formulation included 53 mol. % 1,2-distearoyl-sn-glycero-3-phosphocholine (DSPC, Avanti #850365P), 40 mol. % cholesterol (Avanti #700000P), 2 mol. % Pyro-lipid and 5 mol. % 1,2-distearoyl-sn-glycero-3-phosphoethanolamine-N-[methoxy(polyethylene glycol)-2000 (DSPE-PEG-2K, Avanti #880120P). To generate 100 mg of PoP liposomes (a 5 mL batch), 57.1 mg DSPC, 19.1 mg DSPE-PEG-2K, 2.76 mg Pyro-lipid and 21.1 mg cholesterol were fully dissolved in 1 mL ethanol at 60–70 °C, then 4 mL 250 mM ammonium sulfate (pH 5.5) buffer was injected into the mixed lipids (both mixed lipids and ammonium sulfate buffer were kept at 60–70 °C while injection). Lipids and buffer were fully mixed. The solution was passed 10 times at 60–70 °C through sequentially stacked polycarbonate membranes of 0.2, 0.1 and 0.08 μm pore size using a high pressure nitrogen extruder (Northern Lipids). Free ammonium sulfate was removed by dialysis in a 800 mL solution of 10 % sucrose with 10 mM histidine (pH 6.5) with at least 2 times buffer exchanges.

Cargo loading and release of PoP liposomes

Doxorubicin (Dox; LC Labs # D-4000) was loaded by adding the indicated ratio of drug and incubating at 60 °C for 1 hour. Liposome sizes were determined by dynamic light scattering in PBS. Loading efficiency was determined by running 25 μL of liposomes diluted in 1 mL PBS over a Sephadex G-75 column. 24 × 1 mL fractions were collected and the loading efficiency was determined as the percentage of the drugs in the liposome-containing fractions (which elute in the in the first 3–10 mL). Dox was measured using fluorescence with an excitation of 480 nm and emission of 590 nm using a TECAN Safire fluorescent microplate reader. Light-triggered release experiments were performed using a power-tunable 665 nm laser diode (RPMC laser, LDX-3115-665) at a fluence rate of ~310 mW/cm^2 and Dox release was measured in real time in a fluorometer (PTI). Irradiations were performed in 50% sterile mature bovine serum (Pel-Freez #37218-5) at 37 °C. Temperature was measured by inserting a K-type thermocouple probe directly into the irradiated solution. Dox release was assessed by measuring the release before and after treatment. Release was calculated using the formula $Release=(F_{final}-F_{initial})/(F_{X\text{-}100}-F_{initial})*100\%$.

Cryo-electron microscopy

For cryo-EM, holey carbon grids (c-flat CF-2/2-2C-T) were prepared with an additional layer of continuous thin carbon (5–10 nm) and treated with glow discharge at 5 mA for 15 sec. Then, 3.4 μL of liposome loaded with doxorubicin in buffer containing 10 % sucrose solution and 10 mM histidine (pH 6.5) were applied to the grids for 30 sec. To perform the

specimen vitrification, grids were blotted and plunged in liquid ethane at ~−180 °C using a Vitrobot (FEI) with the blotting chamber maintained at 25 °C and 100% relative humidity. Liposomes were imaged in a JEOL2010F transmission electron microscope at 200kV using a Gatan 914 cryo-holder. Images were collected at x 50,000 magnification and using a total dose of ~20 electrons per Å2 and a defocus range between −7 to −11 microns. Images were recorded in SO-163 films. Micrographs were digitized in a Nikon Super Coolscan 9000 scanner.

Liposome storage stability

Dox loaded stealth PoP Liposomes(drug to lipid molar ratio 1:5) were stored at 4°C in closed amber vials without any other precautions and liposomes were periodically removed for routine analysis. Loading stability, size, polydisperity, serum stability and light triggered release rates were assessed every two weeks for 3 months with 3 separately prepared batches of liposomes. Liposomes sizes were determined in phosphate buffered saline (PBS) by dynamic light scattering. For serum stability measurements, liposomes were diluted 200 times (to 13.5 μg/mL Dox) in PBS containing 50% mature bovine serum (Pel-Freez #37218-5). Initial readings were taken and samples were incubated at 37 °C for 6 hours. 0.5% X-100 was added to lyse the liposomes and final fluorescence value were read. Dox release was calculated according to the formula % Release= $(F_{final}-F_{initial})/(F_{X\text{-}100}-F_{initial})$ ×100%. Loading stability and light triggered release rates were determined as described above.

Pharmacokinetics

All procedures in this work performed on mice were approved by the University at Buffalo Institutional Animal Care and Use Committee. Female mice (female CD-1, 18–20 g, Charles River) were intravenously injected via tail vein with Dox-PoP-liposomes, sterically stabilized liposomal Dox or 10 % HPPH liposomes (10 mol.% HPPH-lipid, 35 mol.% cholesterol, 5 mol.% DSPE-PEG-2K and 50 mol. % DSPC) at dose of 10 mg/kg Dox(N=4 per group). Small blood volumes were sampled at sub-mandibular and retro-orbital locations at the indicated time points. Blood was centrifuged at 2000 x g for 15 minutes. 10 μL serum was added to 990 μL extraction buffer (0.075N HCI, 90% isopropanol) and stored for 20 minutes at −20 °C. The samples were removed and warmed up to room temperature and centrifuged for 15 minutes at 10,000 x g. The supernatants were collected and analyzed by fluorescence. Dox concentrations were determined from standard curves. Noncomparmental pharmacokinetics parameters were analyzed by PKsolver.

Tumor drug uptake

Five week old female nude mice (Jackson Labs, #007850) were inoculated with 5×10^6 MIA Paca-2 cells on both flanks and randomly grouped when the sizes of the tumors reach 6–8 mm (n=4). 1h post i.v. injection with 5mg/kg or 10mg/kg Dox-PoP stealth liposomes, mice were treated 350 mW/cm^2 from a 665 nm laser diode (RPMC laser, LDX-3115-665) for 15min or 30min on one flank. Mice were sacrificed immediately after treatment and tumors were collected. For tumor drug deposition determination, tumors were homogenated in nuclear lysis buffer [0.25 mol/L sucrose, 5 mmol/L Tris-HCl, 1 mmol/l MgSO4,1 mmol/L

$CaCl_2$ (pH 7.6)] and extracted overnight in 0.075N HCI 90% isopropanol. Dox and Pyro-lipid was determined via fluorescence measurements.

Tumor temperature and blood flow

Mice bearing MIA Paca-2 tumors were grouped into 4 groups: Dox-PoP+laser (350 mW/cm^2), Dox-PoP +laser (250 mW/cm^2), laser alone (350 mW/cm^2) and no laser control (n=3–4). Mice in the first two groups were i.v. injected with 7 mg/kg Dox-PoP. 1 hour post injection, mice were anesthetized and placed on a heating pad to maintain body temperature around 35°C. Tumor blood flow were measured by laser Doppler (moorLDI2-IR) in single spot mode. 665 nm laser illumination for phototreatment was initiated 5 minutes after blood flow stabilized. After 30 minutes of illumination, mice were monitored for another 10 minutes. Data were analyzed as % flow rate compared to that of the first five minutes. Tumor temperatures during the treatment courses were recorded by an infrared camera (FLIR ix series).

Survival study

5×10^6 MIA Paca-2 cells (obtained from ATTC) were injected in the right flank female nude mice mice (5 weeks, Jackson Labs, #007850). When tumor volumes reached 4–6 mm in diameter, mice bearing MIA Paca-2 tumors were grouped as follows: 1) Saline control; 2) Dox-PoP-laser;3) Empty PoP+ laser; 4) Dox-PoP+laser. N=5–6. Dose for Dox-PoP is 7mg/kg for Dox and the dose of PoP was adjusted to be equivalent to that of Dox-PoP 7mg/kg (Dox to lipid loading ratio 1:5), which is 1.225mg/kg (1.21μmol/kg Pyro-lipid). For the different dosing experiment, another two groups Dox-PoP+laser (3mg/kg based on Dox) and Dox-PoP+laser (5mg/kg based on Dox) were studied. 21mg/kg of sterically stabilized liposomal Dox (HSPC:CHOL:DSPE-PEG-2K =56.3:38.4:5.3 % mole) was used for standard treatment of Doxil®. Free Dox 7 mg/kg was used as a free drug control. 1 h after intravenous injection, tumors that need laser treatment were all irradiated at a fluence rate of 300 W/cm^2 for 16 min 40s (total fluence 300 J/cm^2). HPPH was diluted in PBS containing 2% ethanol and 0.2% Tween 80 and injected at a dose of 1.21 μmol/kg. Light treatment was performed 24h post injection. Tumor size was monitored 2–3 times per week and tumor volumes were estimated by measuring three tumor dimensions using a caliper and the ellipsoid formula: Volume= $\pi\cdot L\cdot W\cdot H/6$, where L, W and H are the length, width and height of the tumor, respectively. The weights of the mice were monitored every week. MIA paca-2 mice were sacrificed when the volume exceeded 10 times of its initial volume.

Statistical analysis

All data were analyzed by Graphpad prism (Version 5.01) software as indicated in figure captions. For Kaplan-Meier survival curve, each pair of group were compared by Log-rank (Mantel-Cox) test. Bonferroni method is used to adjust for multiple comparisons. Differences were considered significant at $p < 0.05$. Median survival is defined as the time at which the staircase survival curve crosses 50% survival.

Results

Recently we reported that the PoP HPPH-lipid, but not Pyro-lipid, could entrap cargo when liposomes were form with 95 molar % PoP and Dox-loaded liposomes were subsequently prepared with 10 molar % HPPH-lipid PoP.[52] We elected to re-examine Pyro-lipid due to its extreme ease of synthesis and lack of stereocenters. Liposomes were prepared with distearoylphosphocholine (DSPC), Cholesterol (CHOL), DSPE-PEG-2K and Pyro-lipid. 5 molar % DSPE-PEG-2K was included and the remaining lipids were varied as indicated in Figure 1A. Increasing amounts of Pyro-lipid prevented the liposomes from actively loading Dox using an internal ammonium sulfate gradient at 60 °C, an established method for liposomal drug loading.[53] However, this effect could be countered by increasing the cholesterol concentration. Liposomes with higher pyro-lipid concentrations could be loaded by including higher cholesterol concentrations. Liposomes with 30 molar % cholesterol could effectively load Dox, but not when amounts of Pyro-lipid as little as 1 molar % were included in the formulation. With 35 molar % cholesterol, Dox could only be loaded into liposomes containing small amounts of Pyro-lipid (0–2 molar %). The maximal amount of pyro-lipid that could be incorporated in Dox-loaded liposomes increased to 5 and 8 molar % when 40 and 45 molar % cholesterol were included in the formulation, respectively. This phenomenon with relatively abrupt loading behavior was unexpected and was not observed in conventional liposomes lacking Pyro-lipid. As shown in Figure 1B, Dox loading with a relatively high drug to lipid ratio (1:5) was also impacted by the cholesterol content. Unlike conventional liposomes, which loaded Dox in all conditions, PoP liposomes formed with 2 molar % pyro-lipid could only be loaded if more than 35% cholesterol was included. Pyro-lipid PoP liposomes with 45 molar % cholesterol enabled robust active loading of Dox.

To characterize the morphology of the Dox-PoP liposomes cryo-electron microscopy was used. Liposomes were formed with [DSPC:CHOL:PEG-lipid:Pyro-lipid] at a molar ratio of [53:40:5:2] with 1:5 Dox-to-lipid loading ratio. Electron micrographs revealed an unexpected asymmetric structure (Figure 1C). Each Dox-loaded liposome enclosed a prominent electron dense object (indicated by arrows) that was absent from the same liposomes not loaded with Dox (Supporting Figure 1). These were presumably Dox-sulfate precipitates and were typically located off-center. The part of the bilayer near the Dox precipitate had reduced curvature.

Light-triggered release was assessed in vitro with Dox-PoP liposomes at 37 °C in 50% bovine serum. As shown in Figure 2A, increasing amounts of PoP led to faster NIR light-induced release rates, with full release being achieved in a few minutes for most formulations. The fastest times to achieve 50% release occurred in liposomes containing between 2–8 molar % PoP (Figure 2B,C). However when the release rate was normalized to the amount of pyro-lipid in the membrane, 2% pyro-lipid was found to be optimal on a per pyro basis (Figure 2D). In other words, if a set dose of photosensitizer was to be injected, having it in the form of 2 molar % PoP liposomes would result in the greatest amount of light-triggered Dox release. 2% PoP was therefore selected for future experiments since in addition to providing the fastest release per unit PoP, the diminished PoP concentration reduces potential clinical photosensitizer-related side effects such as cutaneous sunlight toxicity.

While increasing cholesterol enabled Dox loading in PoP liposomes (Figure 1), it also slowed the light-triggered Dox release rate. As shown in Figure 3A, PoP liposomes containing 35% cholesterol released Dox the fastest when exposed to NIR laser light whereas those with 50% cholesterol released the slowest. Using less cholesterol to increase release rates was not feasible since it was required to load the Dox into the liposomes. The irradiation time required to induce release of 50% Dox from PoP liposomes showed a clear trend of slower release occurring with increasing cholesterol (Figure 3B), with substantial slowing observed with 50 molar % cholesterol. 40 molar % cholesterol provided the best balance between Dox loading efficiency and rapid light-triggered Dox release.

The effect of DSPE-PEG-2K on Dox loading and triggered release was investigated. PoP liposomes incorporating 45 molar % cholesterol (selected to encourage efficient active loading) and 2 molar % pyro-lipid were formed with varying amounts of DSPE-PEG-2K. As shown in Figure 3C, the time required for 50% Dox release increased from 1.2 min to 2.8 min when 8 molar % of DSPE-PEG-2K was used in place of 3 %. However, DSPE-PEG-2K also played a role in Dox loading, with optimum loading efficiency observed with 5 molar % (Figure 3D), an amount that maintained reasonably fast triggered release (Figure 3C). Thus, after considering each lipid component, PoP liposomes containing DSPC:CHOL:PEG-lipid:PoP with a molar ratio of 53:40:5:2 were finalized as putative stealth PoP liposomes for further evaluation.

We previously developed a formulation with 10 molar % HPPH-lipid, based on the optimal release of calcein.[52] However the optimal amount of HPPH-lipid for the release of actively loaded doxorubicin was found to be 2 molar % (Supporting Figure 2). While HPPH-lipid conferred the conventional stealth liposomes with light-induced release properties, it also led to liposome leakiness. Unlike Pyro-lipid, PoP liposomes formed from HPPH-lipid could not achieve an acceptable balance between serum stability and rapid NIR laser-triggered release (Supporting Figure 3). The developed formulation with 2 molar % Pyro-lipid released contents substantially faster than the previously reported formulation (Supporting Figure 4).

The effect of the drug-to-lipid loading ratio on the encapsulation efficiency, triggered release rates and serum stability at 37 °C of stealth PoP liposomes was next investigated. Figure 4A shows that Dox encapsulation efficiency in PoP liposomes (with 2 molar % Pyro-lipid) with increasing drug-to-lipid loading ratios exhibited a sharp transition point, beyond which drug loading was ineffective. This was in contrast to the same liposomes lacking pyro-lipid, which exhibited gradually decreasing drug encapsulation efficiencies as drug-to-lipid loading ratios increased. The highest drug-to-lipid loading ratio that could be effectively loaded was 1:5 (displayed as 0.2:1 on the graph) and beyond that ratio less than 10% of the Dox could be loaded. For Pyro-lipid PoP liposomes, there was no relationship between the drug loading ratio and the rate of light-triggered drug release and rates of release were highly consistent between all samples (Figure 4B). Figure 4C shows that PoP liposomes with variable loading ratios all exhibited excellent serum stability in vitro. A drug to lipid ratio of 1:5 was selected for further use since it minimizes the amount of injected Pyro-lipid to avoid potential photosensitizer induced side effects.

The long term storage stability of stealth PoP liposomes was evaluated (Fig 1C). The liposomes were stored at 4°C in closed amber vials without any other precautions and liposomes were periodically removed for routine analysis. Loading stability, size, polydisperity, serum stability and light triggered release rates were assessed every two weeks for 3 months with 3 separately prepared batches of liposomes. As shown in Figure 5A, over 95% of the Dox remained stably trapped inside the stealth PoP liposomes. Figure 5B and 5C show that for all separately prepared batches, the size of stealth PoP liposomes remained close to 100 nm, together with a low polydisperity index of close to 0.05, indicating a small and monodisperse population of nanoparticles. Consistently over the storage period, less than 10 % of the loaded Dox leaked from the liposomes when incubated for 6 hours in 50 % bovine serum at 37 °C in vitro (Figure 5D). Thus, for a phototreatment that occurs shortly after intravenous administration of the liposomes, little serum-induced leakage would be predicted to occur. The NIR light-triggered Dox release rate from stealth PoP liposomes remained relatively stable during storage, with close to two minutes of irradiation being required to achieve 50% Dox release (Figure 5E). Thus, despite the high drug-to-lipid loading ratio of 1:5, which gave rise to unusual and asymmetric liposome morphology (Figure 1C), stealth PoP liposomes loaded with Dox exhibited excellent storage stability by all metrics examined. They performed consistently in functional assays for being stable in serum in the absence of NIR light yet quickly releasing contents when exposed to it.

The pharmacokinetic behavior of stealth PoP liposomes loaded with Dox was studied following intravenous administration to CD-1 mice. As shown in Figure 6, encapsulated Dox demonstrated a long-circulating pharmacokinetic profile. The blood elimination time and half-life of Dox in stealth PoP liposomes was close to that of conventional stealth liposomes (containing no Pyro-lipid; equivalent to sterically stabilized liposomal Dox or SSL Dox). Dox-loaded stealth PoP liposomes exhibit a circulating half-life of 21.9 hours with an area under the curve (AUC) of 4837 μg/(ml*h). The half-life of SSL Dox liposomes was 16.9 hours with an area under the curve of 5695 μg/(ml*h). These formulations exhibited substantially greater circulation half lives and AUC than previously reported PoP liposomes that included 10 molar % HPPH-lipid and 35 molar % cholesterol. Table 1 lists pharmacokinetic parameters of Dox-loaded stealth PoP liposomes and other Dox-loaded liposome formulations.

Nude mice were contralaterally inoculated with the human pancreatic MIA Paca-2 cancer cells on both flanks to generate a dual tumor model for light-triggered Dox uptake studies. This method involves one tumor being treated with NIR light and the other serving as a control. Treatment time and injected dose were investigated by measuring Dox tumor uptake immediately after NIR laser treatment. 1 hour following intravenous injection with 5 mg/kg or 10 mg/kg Dox (total intravenously injected Dox dose, encapsulated in stealth PoP liposomes), tumors were laser irradiated for 15 or 30 minutes. Tumor uptake of Dox in the laser irradiated group was 6–7 fold greater than tumors receiving no laser treatment (Figure 7A). The deposition of the drug in tumors was dependent on the injected dose, with the 10 mg/kg injected dose resulting in 13.8 μg Dox per gram of tumor (for the laser treated tumor), which was approximately double the tumor concentration of the 5 mg/kg injected dose (with a laser-treated tumor Dox concentration of 7.0 μg Dox per gram of tumor).

While the injected dose directly impacted light-triggered Dox uptake in the tumor, different light doses (applied using different irradiation times of 15 and 30 minutes) did not have as marked an effect. Mice treated with an injected dose of 10 mg/kg and irradiated for either 15 or 30 minutes resulted in 9.6 and 13.2 μg Dox per gram in laser-treated tumor tissue, respectively, and these were not statistically significantly different (Figure 7B). Further research is required to better understand the impact of different light doses, but laser treatment could possibly be inducing partial vascular stasis, preventing more liposomes flowing into the tumors.

The effect of laser treatment on the tumor temperature was examined (Figure 8A). One hour after 7 mg/kg Dox dosing, laser irradiation was applied at 350 mW/cm^2 and caused the surface temperature of the tumor to increase up to 45 °C over 30 minutes of irradiation. When the fluence rate was lowered to 250 mW/cm^2, the temperature increased to less than 40 °C. This rise in temperature was similar to the observed tumor surface heating when 350 mW/cm^2 was applied, without the prior injection of PoP liposomes. Tumor blood flow was assessed with laser Doppler analysis, a technique which can non-invasively probe superficial perfusion in the investigated tissue. As shown in Figure 8B, in the absence of PoP-liposomes, tumor blood flow was not inhibited by the 350 mW/cm^2 laser treatment, and increased over time by approximately 50%, possibly due to thermal heating effects. Tumors irradiated when stealth PoP liposomes were circulating in blood exhibited drastically different blood flow dynamics (Figure 8C). Tumor blood flow initially decreased sharply, followed by an increase and then a subsequent decrease. This trend was observed at both 250 mW/cm^2 and 350 mW/cm^2 fluence rates. Vascular shutdown continued after the laser was turned off following 30 minutes of irradiation. The decrease in blood flow during laser irradiation was not due to tumor heating, since the 250 mW/cm^2 treatment resulted in similar heating to the drug-free 350 mW/cm^2 treatment, which did not show any vascular shutdown (Figure 8B). The phenomenon of an immediate decreasing tumor flow, followed by a subsequent increase has been reported in mice with high fluence photodynamic therapy (PDT).[54] When plotted as a function of cumulative fluence, the 250 mW/cm^2 and 350 mW/cm^2 treatments exhibited similar patterns of tumor vascular dynamics (Figure 8D).

The anti-tumor efficacy of Dox stealth PoP liposomes was assessed in nude mice bearing single MIA Paca-2 subcutaneous tumors. As shown in Figure 9A, at a dose of 7 mg/kg Dox (or equivalent) both Dox-loaded stealth PoP liposomes alone (without laser treatment) and unloaded stealth PoP liposome with laser treatment provided some therapeutic benefit by prolonging median survival times compared to untreated control mice from 21 days to 30.5 days for both groups. However, a strong therapeutic synergy was observed for Dox-loaded stealth PoP liposomes with laser treatment, as this approach led to full survival of all mice and was significantly more effective than the two aforementioned control treatments ($P<0.05$). With a 7 mg/kg dose of Dox in stealth PoP liposomes, all phototreated tumors effectively regressed to less than 20 mm^3 within two weeks of treatment and all mice survived the duration of the study (60 days) with 3 of 6 tumors permanently cured. The phototherapeutic efficacy of Dox-loaded stealth PoP liposomes at lower doses was examined (Figure 9B). Both 3 mg/kg and 5 mg/kg Dox were highly effective in delaying tumor growth. Laser treated mice treated with Dox-PoP liposomes had a median survival time of 43.5 days with 3 mg/kg Dox, and 57 days with 5 mg/kg Dox. For mice treated with 5 mg/kg

Dox, tumor regrowth was seen in only 3 of 6 mice. In all cases, Dox-loaded stealth PoP liposome phototreatments were well tolerated, as evidenced by healthy body mass in all treated mice (Figure 9C).

As shown in Figure 9D, phototreatment with Dox-loaded stealth PoP liposomes was substantially more effective than single-dose treatments of conventional chemotherapy or PDT. Free Dox, at its maximum tolerated dose of 7 mg/kg was ineffective treatment against MIA Paca-2 tumors, with no significant tumor growth delay compared to control mice (median survival 19 vs 21 days). Sterically stabilized Dox (SSL Dox) could be administered at a three times higher maximum tolerated dose compared to the free drug, and improved survival compared to control (median survival 40 days vs 21 days, $P<0.05$). Conventional PDT exhibited a similar tumor growth inhibition (median survival 38 days) when administered with an equivalent light dose and equivalent injected dose of HPPH, a photosensitizer with similar spectral properties as Pyro-lipid and currently in clinical trials. Dox-loaded stealth PoP liposomes with laser treatment was significantly more effective than these three anti-cancer modalities which have all been used in the clinic. Standard treatment of SSL Dox at a high dose (21 mg/kg) later on developed rashes on the feet of the mice which is typical symptom of palmar-plantar erythrodysesthesia (PPE) at high dose of stealth liposomal doxorubicin.[55,56] Tumor volumes revealed that all Dox phototreatments with stealth PoP liposomes were more efficacious than the maximum tolerated doses of free and SSL Dox (Figure 9E). Stealth PoP liposome phototreatment with 3 mg/kg Dox was slightly more effective than SSL Dox at 21 mg/kg. Even with presumed faster blood clearance observed with lower injected doses of liposome, PoP liposomes can be used at least 7 times lower dosage with superior therapeutic efficacy to conventional SSL Dox. These results are encouraging for achieving tumor ablation with minimal side effects.

Discussion

In this study, we systematically examined all lipid components of PoP liposomes to successfully develop a formulation that 1) could be actively loaded with Dox with high efficacy and loading ratios; 2) was stable in vitro during storage and in serum; 3) had long circulating times in vivo; and 4) could rapidly release Dox when exposed to NIR light. Increasing amounts of cholesterol enabled active loading with increasing amounts of PoP, which itself tended to destabilize the bilayer and prevent Dox loading. Although cholesterol is known to enhance liposome stability[57,58], further studies are required to better determine the role cholesterol plays in the function and structure of PoP liposomes. Increasing amounts of cholesterol also slowed down light-triggered Dox release, as did DSPE-PEG-2K. However both components were required for effective Dox loading. High Dox-to-lipid loading ratios (1:5) were possible and gave rise to unusual liposomal morphology as demonstrated in Fig 1C. How cholesterol and DSPE-PEG-2K slows light triggered drug release is of interest and further elucidation of mechanistic aspects is required.

Increasing amounts of Pyro-lipid inhibited the loading of Dox into PoP liposomes, an effect which had to be countered by increasing the cholesterol content. Increased Pyro-lipid also increased the light-triggered release rate. An optimal amount of 2 molar % Pyro was selected since this gave the most rapid release rate when normalized by the amount of Pyro-

lipid in the bilayer. Although Pyro-lipid has been shown to be well-tolerated in mice at intravenous doses as high as 1 g/kg[43], administration of lower doses of molecules that are photosensitizers to patients is preferred to avoid undesired sunlight toxicity or edema formation in the irradiated area as observed in PDT treatment.[59] Using the developed Dox-loaded stealth PoP liposome formulation, Dox dosing at a low human dose of 5 mg/m^2, would correspond to PoP dosing in the ballpark of 1 mg/m^2 or 0.03 mg/kg, a photosensitizer dose that is orders of magnitude less than clinically approved Photofrin, which is usually administered at 2 mg/kg doses.

Immediately following laser treatment, a 6–7 fold increase of tumor uptake of doxorubicin was observed. The striking increase in tumoral drug concentration is likely an important factor for the effectiveness of this treatment. The enhanced drug accumulation can be due to a combination of drug release, hyperthermia-mediated vessel permeabilization, and also PDT-induced vascular permeability effect. Both triggered release[13,21] and PDT[60,61] can be used as means to enhance drug delivery. Further studies are needed to thoroughly ascertain the contributions of each mechanism on enhanced drug uptake and enhanced bioavailability. When treatment time with 350 mW/cm^2 irradiation was increased from 15 to 30 minutes, tumor drug uptake increased, but not with statistical significance. As shown in Figure 8C, after 20 minutes of irradiation, blood flow decreased in the tumor, limiting the amount of drug that could be deposited. PDT induced microvascular stasis was likely occurring and inhibiting further supply of liposomes to the irradiated volumes.[62,63] For tumor growth inhibition studies, a 16.7 minute treatment was performed with an intermediate fluence rate of 300 mW/cm^2, so that tumor heating did not exceed 43 °C, and intra-treatment vascular shutdown during was minimal. Future directions include combining this treatment with anticoagulants, which might reduce PDT-induced vascular stasis and further improve tumor drug uptake.

Conclusion

We systematically developed a robust sterically-stabilized, long-circulating stealth PoP liposome formulation which can be triggered by NIR light to release encapsulated drugs. Dox-loaded stealth PoP liposomes exhibited long term storage stability. PoP liposome chemophototherapy anti-tumor efficacy was superior to conventional PDT (using HPPH) and to a maximum tolerated single dose of Dox, administered freely or in long-circulating liposomes. A combination of enhanced drug deposition, mild tumor heating, vascular photodynamic effects and drug release likely play roles in treatment efficacy.

Supplementary Material

Refer to Web version on PubMed Central for supplementary material.

Acknowledgments

This work was supported by the National Institutes of Health (R01EB017270, DP5OD017898 and R21EB019147).

References

1. Needham D, Dewhirst MW. The Development and Testing of a New Temperature-Sensitive Drug Delivery System for the Treatment of Solid Tumors. Adv Drug Deliv Rev. 2001; 53:285–305. [PubMed: 11744173]
2. Allen TM, Cullis PR. Drug Delivery Systems: Entering the Mainstream. Science. 2004; 303:1818–1822. [PubMed: 15031496]
3. Shum P, Kim JM, Thompson DH. Phototriggering of Liposomal Drug Delivery Systems. Adv Drug Deliv Rev. 2001; 53:273–284. [PubMed: 11744172]
4. Luo D, Carter KA, Lovell JF. Nanomedical Engineering: Shaping Future Nanomedicines. Wiley Interdiscip Rev Nanomed Nanobiotechnol. 2015; 7:169–188. [PubMed: 25377691]
5. Allen TM, Cullis PR. Drug Delivery Systems: Entering the Mainstream. Science. 2004; 303:1818–1822. [PubMed: 15031496]
6. Torchilin VP. Recent Advances with Liposomes as Pharmaceutical Carriers. Nat Rev Drug Discov. 2005; 4:145. [PubMed: 15688077]
7. Papahadjopoulos D, Allen TM, Gabizon A, Mayhew E, Matthay K, Huang SK, Lee KD, Woodle MC, Lasic DD, Redemann C. Sterically Stabilized Liposomes: Improvements in Pharmacokinetics and Antitumor Therapeutic Efficacy. Proc Natl Acad Sci. 1991; 88:11460–11464. [PubMed: 1763060]
8. Klibanov AL, Maruyama K, Torchilin VP, Huang L. Amphipathic Polyethyleneglycols Effectively Prolong the Circulation Time of Liposomes. FEBS Lett. 1990; 268:235–237. [PubMed: 2384160]
9. Gabizon AA, Barenholz Y, Bialer M. Prolongation of the Circulation Time of Doxorubicin Encapsulated in Liposomes Containing a Polyethylene Glycol-Derivatized Phospholipid: Pharmacokinetic Studies in Rodents and Dogs. Pharm Res. 1993; 10:703–708. [PubMed: 8321835]
10. Gabizon A, Catane R, Uziely B, Kaufman B, Safra T, Cohen R, Martin F, Huang A, Barenholz Y. Prolonged Circulation Time and Enhanced Accumulation in Malignant Exudates of Doxorubicin Encapsulated in Polyethylene-Glycol Coated Liposomes. Cancer Res. 1994; 54:987–992. [PubMed: 8313389]
11. Rivera E, Valero V, Esteva FJ, Syrewicz L, Cristofanilli M, Rahman Z, Booser DJ, Hortobagyi GN. Lack of Activity of Stealth Liposomal Doxorubicin in the Treatment of Patients with Anthracycline-Resistant Breast Cancer. Cancer Chemother Pharmacol. 2002; 49:299–302. [PubMed: 11914909]
12. O'Brien MER, Wigler N, Inbar M, Rosso R, Grischke E, Santoro A, Catane R, Kieback DG, Tomczak P, Ackland SP, et al. Reduced Cardiotoxicity and Comparable Efficacy in a Phase III Trial of Pegylated Liposomal Doxorubicin HCl (CAELYX$_{TM}$/Doxil®) versus Conventional Doxorubicin for First-Line Treatment of Metastatic Breast Cancer. Ann Oncol. 2004; 15:440–449. [PubMed: 14998846]
13. Kong G, Anyarambhatla G, Petros WP, Braun RD, Colvin OM, Needham D, Dewhirst MW. Efficacy of Liposomes and Hyperthermia in a Human Tumor Xenograft Model: Importance of Triggered Drug Release. Cancer Res. 2000; 60:6950–6957. [PubMed: 11156395]
14. Schroeder A, Honen R, Turjeman K, Gabizon A, Kost J, Barenholz Y. Ultrasound Triggered Release of Cisplatin from Liposomes in Murine Tumors. J Controlled Release. 2009; 137:63–68.
15. Timko BP, Dvir T, Kohane DS. Remotely Triggerable Drug Delivery Systems. Adv Mater. 2010; 22:4925–4943. [PubMed: 20818618]
16. Ganta S, Devalapally H, Shahiwala A, Amiji M. A Review of Stimuli-Responsive Nanocarriers for Drug and Gene Delivery. J Controlled Release. 2008; 126:187–204.
17. Drummond DC, Zignani M, Leroux JC. Current Status of pH-Sensitive Liposomes in Drug Delivery. Prog Lipid Res. 2000; 39:409–460. [PubMed: 11082506]
18. Simões S, Moreira JN, Fonseca C, Düzgüneş N, Pedroso de Lima MC. On the Formulation of pH-Sensitive Liposomes with Long Circulation Times. Adv Drug Deliv Rev. 2004; 56:947–965. [PubMed: 15066754]
19. Felber AE, Dufresne MH, Leroux JC. pH-Sensitive Vesicles, Polymeric Micelles, and Nanospheres Prepared with Polycarboxylates. Adv Drug Deliv Rev. 2012; 64:979–992. [PubMed: 21996056]

20. Leroux JC, Roux E, Le Garrec D, Hong K, Drummond DC. N-Isopropylacrylamide Copolymers for the Preparation of pH-Sensitive Liposomes and Polymeric Micelles. J Controlled Release. 2001; 72:71–84.
21. Needham D, Anyarambhatla G, Kong G, Dewhirst MW. A New Temperature-Sensitive Liposome for Use with Mild Hyperthermia: Characterization and Testing in a Human Tumor Xenograft Model. Cancer Res. 2000; 60:1197–1201. [PubMed: 10728674]
22. Lindner LH, Eichhorn ME, Eibl H, Teichert N, Schmitt-Sody M, Issels RD, Dellian M. Novel Temperature-Sensitive Liposomes with Prolonged Circulation Time. Clin Cancer Res Off J Am Assoc Cancer Res. 2004; 10:2168–2178.
23. Basel MT, Shrestha TB, Troyer DL, Bossmann SH. Protease-Sensitive, Polymer-Caged Liposomes: A Method for Making Highly Targeted Liposomes Using Triggered Release. ACS Nano. 2011; 5:2162–2175. [PubMed: 21314184]
24. de la Rica R, Aili D, Stevens MM. Enzyme-Responsive Nanoparticles for Drug Release and Diagnostics. Adv Drug Deliv Rev. 2012; 64:967–978. [PubMed: 22266127]
25. Alvarez-Lorenzo C, Bromberg L, Concheiro A. Light-SensiMve Intelligent Drug Delivery Systems†. Photochem Photobiol. 2009; 85:848–860. [PubMed: 19222790]
26. Carter KA, Shao S, Hoopes MI, Luo D, Ahsan B, Grigoryants VM, Song W, Huang H, Zhang G, Pandey RK, et al. Porphyrin–phospholipid Liposomes Permeabilized by near-Infrared Light. Nat Commun. 2014; 5
27. Podaru G, Ogden S, Baxter A, Shrestha T, Ren S, Thapa P, Dani RK, Wang H, Basel MT, Prakash P, et al. Pulsed Magnetic Field Induced Fast Drug Release from Magneto Liposomes via Ultrasound Generation. J Phys Chem B. 2014; 118:11715–11722. [PubMed: 25110807]
28. Landon CD, Park JY, Needham D, Dewhirst MW. Nanoscale Drug Delivery and Hyperthermia: The Materials Design and Preclinical and Clinical Testing of Low Temperature-Sensitive Liposomes Used in Combination with Mild Hyperthermia in the Treatment of Local Cancer. Open Nanomedicine J. 2011; 3:38–64.
29. Mura S, Nicolas J, Couvreur P. Stimuli-Responsive Nanocarriers for Drug Delivery. Nat Mater. 2013; 12:991–1003. [PubMed: 24150417]
30. Rai P, Mallidi S, Zheng X, Rahmanzadeh R, Mir Y, Elrington S, Khurshid A, Hasan T. Development and Applications of Photo-Triggered Theranostic Agents. Adv Drug Deliv Rev. 2010; 62:1094–1124. [PubMed: 20858520]
31. You J, Zhang G, Li C. Exceptionally High Payload of Doxorubicin in Hollow Gold Nanospheres for Near-Infrared Light-Triggered Drug Release. ACS Nano. 2010; 4:1033–1041. [PubMed: 20121065]
32. Ma Y, Liang X, Tong S, Bao G, Ren Q, Dai Z. Gold Nanoshell Nanomicelles for Potential Magnetic Resonance Imaging, Light-Triggered Drug Release, and Photothermal Therapy. Adv Funct Mater. 2013; 23:815–822.
33. Yang X, Liu X, Liu Z, Pu F, Ren J, Qu X. Near-Infrared Light-Triggered, Targeted Drug Delivery to Cancer Cells by Aptamer Gated Nanovehicles. Adv Mater. 2012; 24:2890–2895. [PubMed: 22539076]
34. Fomina N, Sankaranarayanan J, Almutairi A. Photochemical Mechanisms of Light-Triggered Release from Nanocarriers. Adv Drug Deliv Rev. 2012; 64:1005–1020. [PubMed: 22386560]
35. Carling CJ, Viger ML, Huu VAN, Garcia AV, Almutairi A. In Vivo Visible Light-Triggered Drug Release From an Implanted Depot. Chem Sci R Soc Chem 2010. 2015; 6:335–341.
36. Timko BP, Arruebo M, Shankarappa SA, McAlvin JB, Okonkwo OS, Mizrahi B, Stefanescu CF, Gomez L, Zhu J, Zhu A, et al. Near-Infrared–actuated Devices for Remotely Controlled Drug Delivery. Proc Natl Acad Sci. 2014; 111:1349–1354. [PubMed: 24474759]
37. Dvir T, Banghart MR, Timko BP, Langer R, Kohane DS. Photo-Targeted Nanoparticles. Nano Lett. 2010; 10:250–254. [PubMed: 19904979]
38. Melancon MP, Zhou M, Li C. Cancer Theranostics with Near-Infrared Light-Activatable Multimodal Nanoparticles. Acc Chem Res. 2011; 44:947–956. [PubMed: 21848277]
39. Timko BP, Kohane DS. Prospects for near-Infrared Technology in Remotely Triggered Drug Delivery. Expert Opin Drug Deliv. 2014; 11:1681–1685. [PubMed: 25008774]

40. Yatvin M, Weinstein J, Dennis W, Blumenthal R. Design of Liposomes for Enhanced Local Release of Drugs by Hyperthermia. Science. 1978; 202:1290–1293. [PubMed: 364652]
41. Weinstein JN, Magin RL, Yatvin MB, Zaharko DS. Liposomes and Local Hyperthermia: Selective Delivery of Methotrexate to Heated Tumors. Science. 1979; 204:188–191. [PubMed: 432641]
42. Ishida O, Maruyama K, Yanagie H, Eriguchi M, Iwatsuru M. Targeting Chemotherapy to Solid Tumors with Long-Circulating Thermosensitive Liposomes and Local Hyperthermia. Jpn J Cancer Res Gann. 2000; 91:118–126. [PubMed: 10744053]
43. Lovell JF, Jin CS, Huynh E, Jin H, Kim C, Rubinstein JL, Chan WCW, Cao W, Wang LV, Zheng G. Porphysome Nanovesicles Generated by Porphyrin Bilayers for Use as Multimodal Biophotonic Contrast Agents. Nat Mater. 2011; 10:324–332. [PubMed: 21423187]
44. Rieffel J, Chen F, Kim J, Chen G, Shao W, Shao S, Chitgupi U, Hernandez R, Graves SA, Nickles RJ, et al. Hexamodal Imaging with Porphyrin-Phospholipid-Coated Upconversion Nanoparticles. Adv Mater. 2015; 27:1785–1790. [PubMed: 25640213]
45. Zhang Y, Lovell JF. Porphyrins as Theranostic Agents from Prehistoric to Modern Times. Theranostics. 2012; 2:905–915. [PubMed: 23082102]
46. Huang H, Song W, Rieffel J, Lovell JF. Emerging Applications of Porphyrins in Photomedicine. Biomed Phys. 2015; 3:23.
47. Shao S, Geng J, Ah Yi H, Gogia S, Neelamegham S, Jacobs A, Lovell JF. Functionalization of Cobalt Porphyrin–phospholipid Bilayers with His-Tagged Ligands and Antigens. Nat Chem. 2015; 7:438–446. [PubMed: 25901823]
48. He C, Liu D, Lin W. Self-Assembled Core–Shell Nanoparticles for Combined Chemotherapy and Photodynamic Therapy of Resistant Head and Neck Cancers. ACS Nano. 2015; 9:991–1003. [PubMed: 25559017]
49. Ferrario A, Gomer CJ. Systemic Toxicity in Mice Induced by Localized Porphyrin Photodynamic Therapy. Cancer Res. 1990; 50:539–543. [PubMed: 2137023]
50. Veenhuizen RB, Ruevekamp-Helmers MC, Helmerhorst TJM, Kenemans P, Mooi WJ, Marijnissen JPA, Stewart FA. Intraperitoneal Photodynamic Therapy in the Rat: Comparison of Toxicity Profiles for Photofrin and mTHPC. Int J Cancer. 1994; 59:830–836. [PubMed: 7989125]
51. Wooten RS, Smith KC, Ahlquist DA, Muller SA, Balm RK. Prospective Study of Cutaneous Phototoxicity after Systemic Hematoporphyrin Derivative. Lasers Surg Med. 1988; 8:294–300. [PubMed: 2969070]
52. Carter KA, Shao S, Hoopes MI, Luo D, Ahsan B, Grigoryants VM, Song W, Huang H, Zhang G, Pandey RK, et al. Porphyrin–phospholipid Liposomes Permeabilized by near-Infrared Light. Nat Commun. 2014; 5
53. Haran G, Cohen R, Bar LK, Barenholz Y. Transmembrane Ammonium Sulfate Gradients in Liposomes Produce Efficient and Stable Entrapment of Amphipathic Weak Bases. Biochim Biophys Acta BBA - Biomembr. 1993; 1151:201–215.
54. Rohrbach DJ, Tracy EC, Walker J, Baumann H, Sunar U. Blood Flow Dynamics during Local Photoreaction in a Head and Neck Tumor Model. Biomed Phys. 2015; 3:13.
55. Lorusso D, Stefano AD, Carone V, Fagotti A, Pisconti S, Scambia G. Pegylated Liposomal Doxorubicin-Related Palmar-Plantar Erythrodysesthesia (“hand-Foot” Syndrome). Ann Oncol. 2007; 18:1159–1164. [PubMed: 17229768]
56. Lopez AM, Wallace L, Dorr RT, Koff M, Hersh EM, Alberts DS. Topical DMSO Treatment for Pegylated Liposomal Doxorubicin-Induced Palmar-Plantar Erythrodysesthesia. Cancer Chemother Pharmacol. 1999; 44:303–306. [PubMed: 10447577]
57. Gregoriadis G, Davis C. Stability of Liposomes Invivo and Invitro Is Promoted by Their Cholesterol Content and the Presence of Blood Cells. Biochem Biophys Res Commun. 1979; 89:1287–1293. [PubMed: 496958]
58. Kirby C, Clarke J, Gregoriadis G. Effect of the Cholesterol Content of Small Unilamellar Liposomes on Their Stability in Vivo and in Vitro. Biochem J. 1980; 186:591–598. [PubMed: 7378067]
59. Li LB, Luo RC. Effect of Drug-Light Interval on the Mode of Action of Photofrin Photodynamic Therapy in a Mouse Tumor Model. Lasers Med Sci. 2009; 24:597–603. [PubMed: 18936869]

60. Snyder JW, Greco WR, Bellnier DA, Vaughan L, Henderson BW. Photodynamic Therapy: A Means to Enhanced Drug Delivery to Tumors. Cancer Res. 2003; 63:8126–8131. [PubMed: 14678965]

61. Chen B, Pogue BW, Luna JM, Hardman RL, Hoopes PJ, Hasan T. Tumor Vascular Permeabilization by Vascular-Targeting Photosensitization: Effects, Mechanism, and Therapeutic Implications. Clin Cancer Res. 2006; 12:917–923. [PubMed: 16467106]

62. Chen B, Pogue BW, Goodwin IA, O'Hara JA, Wilmot CM, Hutchins JE, Jack Hoopes P, Hasan T. Blood Flow Dynamics after Photodynamic Therapy with Verteporfin in the RIF-1 Tumor. Radiat Res. 2003; 160:452–459. [PubMed: 12968929]

63. Fingar VH. Vascular Effects of Photodynamic Therapy. J Clin Laser Med Surg. 1996; 14:323–328. [PubMed: 9612199]

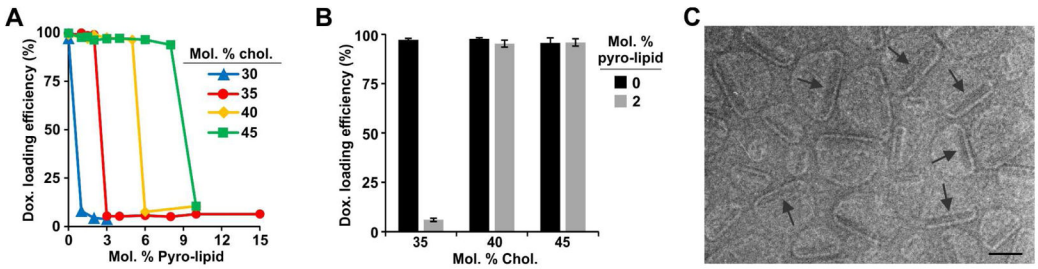

Figure 1. Cholesterol enables Dox loading into PoP liposomes

A) Dox active loading efficiency in PoP liposomes with a Dox-to-lipid loading molar ratio of 1:8. 5 mol. % PEG-lipid was included together with the indicated amounts cholesterol and Pyro-lipid, and DSPC completed the formulation. **B)** Dox active loading efficiency in liposomes with or without 2 molar % pyro-lipid. The Dox-to-lipid loading molar ratio was 1:5. Values show mean +/− S.D. for n=3. **C)** Cryo-electron micrographs of Dox-PoP liposomes formed with a DSPC:CHOL:PEG-lipid:PoP molar ratio of 53:40:5:2 and a 1:5 Dox-to-lipid loading ratio. Images were collected with a defocus ranging between −7 to −8 microns defocus. Arrows point to Dox precipitates within the liposomes. 100 nm scale bar is shown.

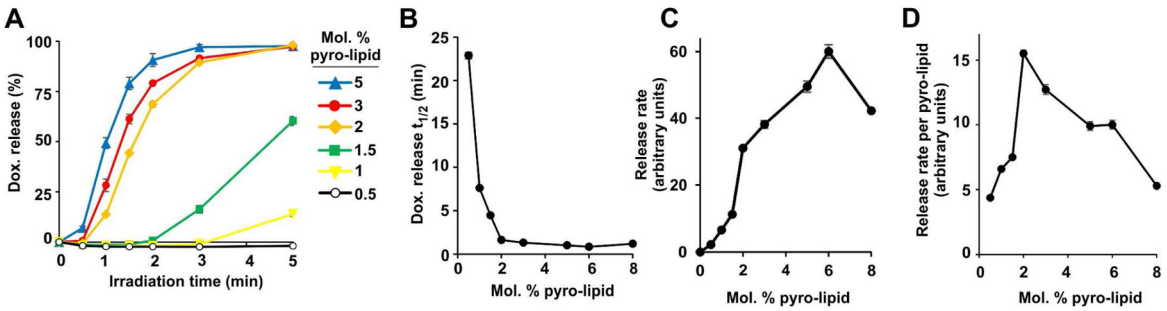

Figure 2. Effect of PoP concentration on the rate of light-triggered Dox release

A) Real-time Dox release from PoP liposomes during 665 nm laser irradiation with varying amounts of Pyro-lipid incorporated. No detectable release occurs without laser irradiation. **B)** Laser irradiation time required for PoP liposomes to release 50% of the loaded Dox. **C)** Light-induced Dox release rate for PoP liposomes. **D)** Light-induced Dox release rate normalized by the amount of Pyro-lipid. Data show mean +/−S.D. for n=3. All measurements were recorded in 50 % bovine serum at 37 °C.

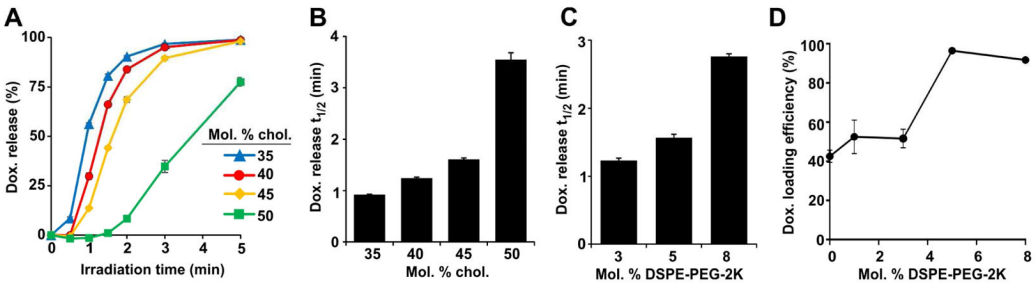

Figure 3. Cholesterol and DSPE-PEG-2K slow light-triggered release from PoP liposomes

A) Real-time Dox release during 665 nm laser irradiation from PoP liposomes containing 2 molar % Pyro-lipid with varying amounts of cholesterol. Laser irradiation time required for PoP liposomes to release 50% of loaded Dox as a function of incorporated **B)** Cholesterol or **C)** DSPE-PEG-2K. Light-triggered release measurements were recorded in 50 % bovine serum at 37 °C. **D)** Dox active loading efficiency in liposomes made with varying amounts of DSPE-PEG-2K using a 1:5 Dox-to-lipid molar ratio. All data show mean +/− S.D. for n=3.

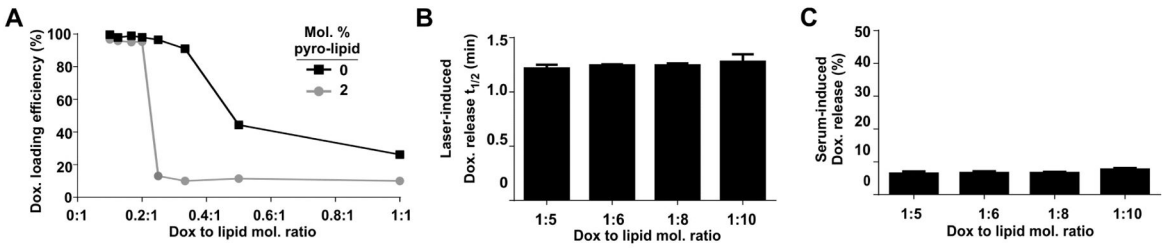

Figure 4. Dox-to-lipid loading ratios do not impact stealth PoP liposome light-triggered release rates or in vitro serum stability

Stealth PoP liposomes were formed with DSPC:CHOL:DSPE-PEG-2K:PoP with molar ratios of 53:40:5:2. **A)** Dox active loading efficiency in liposomes with or without 2 molar % Pyro-lipid at varying drug-to-lipid molar ratios. **B**) Laser irradiation time required for stealth PoP liposomes to release 50% of loaded Dox as a function of Dox-to-lipid molar ratio. **C)** Serum stability of stealth PoP liposomes loaded at the indicated Dox-to-lipid molar ratios in 50% bovine serum, incubated at 37 °C for 4 hours. Mean+/−S.D., n=3.

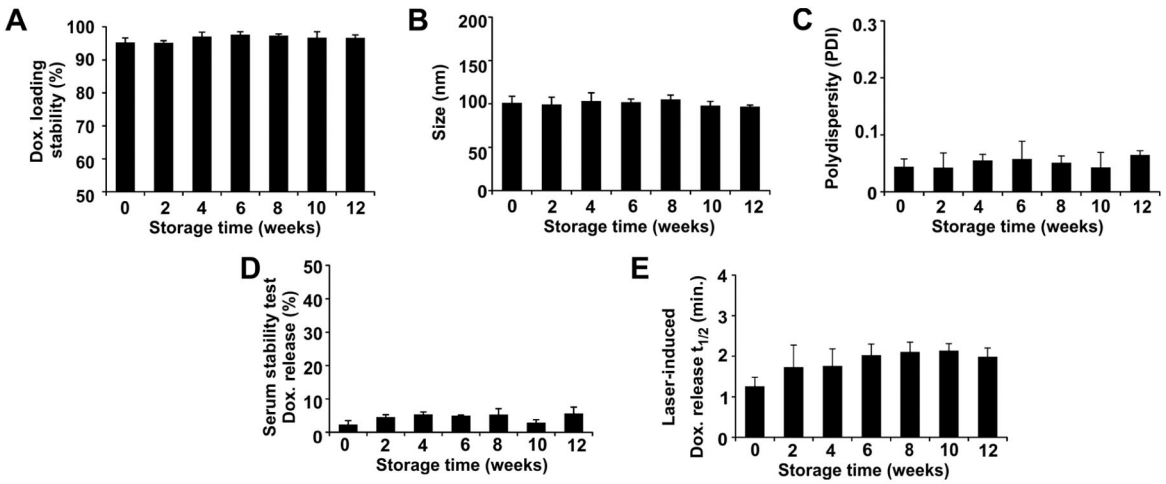

Figure 5. Storage stability of Dox-loaded stealth PoP liposomes

Liposomes were stored at 4 °C. **A)** Dox retention; **B)** liposome size; and **C)** liposome polydisperity. **D)** In vitro serum stability of loaded Dox following 6 hours incubation at 37 °C in 50 % bovine serum. **E)** Laser irradiation time required for release 50% of loaded Dox in 50 % bovine serum at 37 °C. Data show mean +/− S.D. for n=3 separately prepared batches of liposomes.

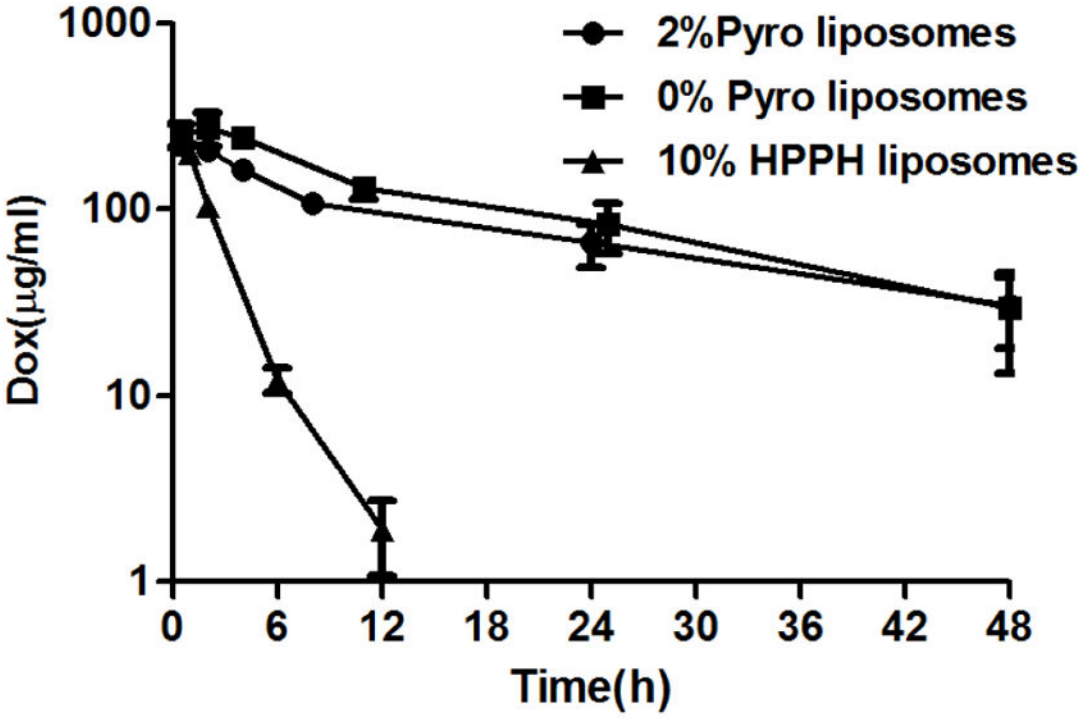

Figure 6. Long blood circulation of Dox loaded in stealth PoP liposomes

Serum concentration of Dox loaded in indicated liposomes and intravenously administered to CD-1 mice. Values show mean +/− S.D. for n=4–5 mice per group.

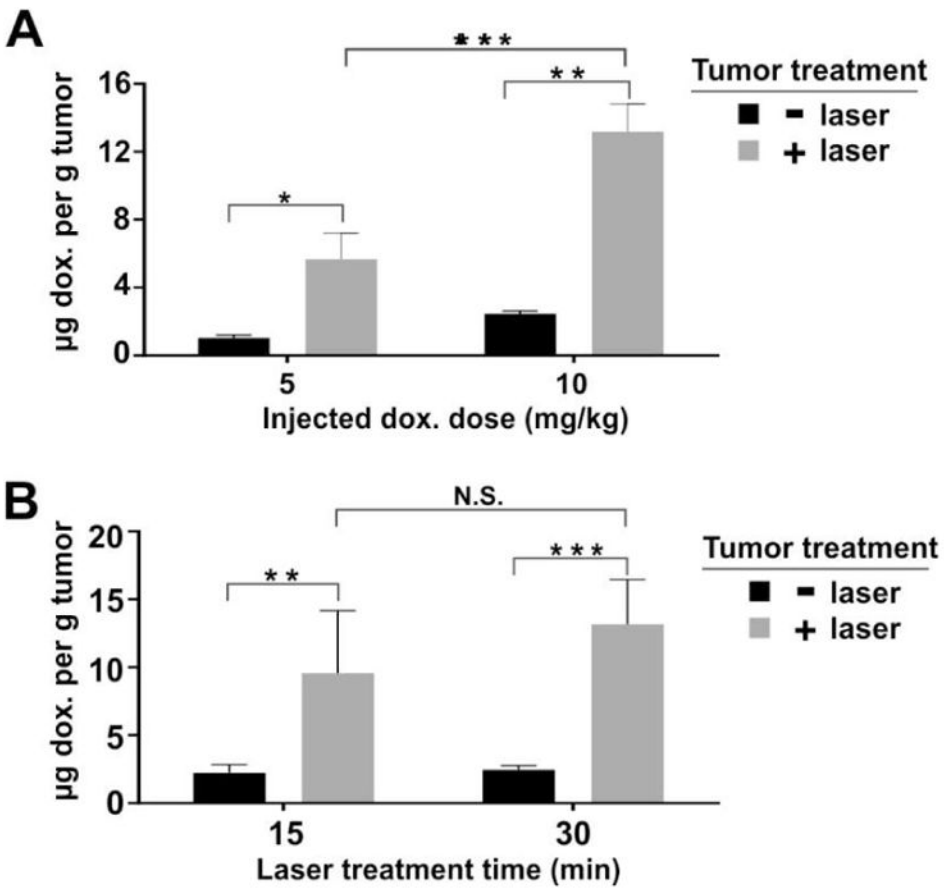

Figure 7. Laser-induced enhanced Dox deposition from stealth PoP liposomes in a contralateral Mia Paca-2 dual tumor model

1 hour after intravenous injection of Dox-loaded stealth PoP liposomes, tumors on only one flank of the mice were irradiated with a 665 nm laser. Immediately after irradiation, mice were sacrificed and Dox concentration in both treated and untreated tumors was determined. **A)** Effect of injected dose of 5 mg/kg or 10 mg/kg Dox in stealth PoP liposomes. Tumors were treated with 30 minutes of 665 nm irradiation at 350 mW/cm^2. **B)** Effect of different irradiation times of 15 or 30 minutes. Mice were injected with 10 mg/kg Dox in stealth PoP liposomes and tumors were treated with 665 nm irradiation at 350 mW/cm^2. There was no significant difference between 15 and 30 minutes irradiation time in terms of tumor Dox uptake. Statistical analysis were performed by Bonferroni post-test, two way ANOVA,*P<0.05, ** P<0.01, ***P<0.001. Mean +/− S.D. for n=4 tumors per group.

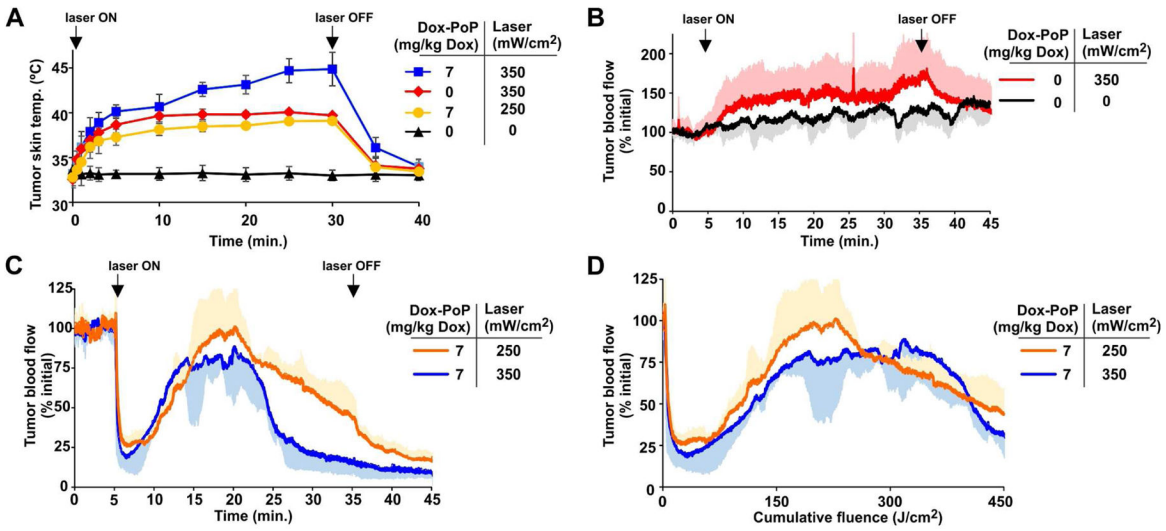

Figure 8. Tumor surface temperature and blood flow during phototreatment with stealth PoP liposomes

A) Surface temperature of MIA Paca-2 xenograft during treatment with a 665 nm laser diode at indicated power one hour after intravenous administration of PoP liposomes at the indicated Dox dose. **B)** Relative change in tumor blood flow induced by the laser treatment itself. Laser was switched on at indicated fluence rate as indicated. **C**, **D**) Relative change in tumor blood flow as a function of time (C) or cumulative fluence (D) for mice one hour after intravenous administration of stealth PoP liposomes at the indicated laser fluence rates. Values indicate mean with S.D. (in a single vertical direction for blood flow data) for n=3–4 mice per group.

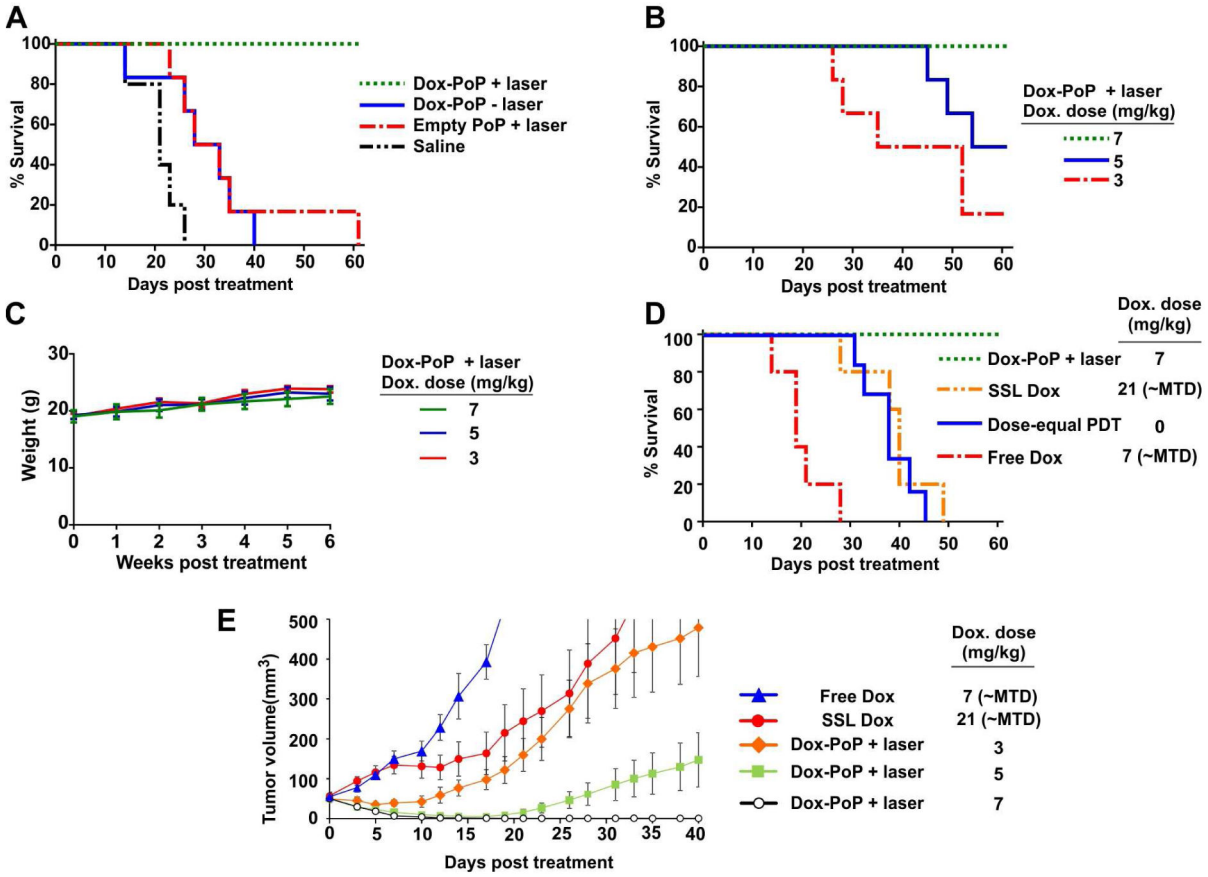

Figure 9. Phototreatment efficacy of Dox-loaded stealth PoP liposomes

Nude mice bearing MIA Paca-2 tumors were treated when tumor diameter reached 4–5 mm and were sacrificed when tumor volume increased 10 fold. Laser treatments involved administration of 300 J/cm^2 of 665 nm light (300 mW/cm^2 over 16.7 minutes). **A)** Synergistic efficacy of Dox stealth PoP liposomes with laser treatment. Dox was administered at 7 mg/kg or with equivalent dosage in control groups. **B)** Dose response of Dox-loaded stealth PoP liposomes with phototreatment. The examined doses of 3, 5, 7 mg/kg were significantly more effective than untreated control groups ($P<0.05$). **C)** Body mass of mice that were phototreated with Dox-loaded stealth PoP liposomes. **D)** Dox-loaded stealth PoP liposomes with phototreatment were significantly more effective than conventional anti-tumor treatments including SSL Dox and free Dox at their maximum tolerated dose (MTD) or conventional PDT using HPPH at with the same light treatment and an equivalent photosensitizer dose ($P<0.05$). **E)** Tumor volume growth for indicated treatment groups. Mean +/− S.E. for n=5–6 mice per group.

Table 1

Noncompartmental pharmacokinetics analysis of liposomal Dox

	$T_{1/2}$(h)	C_{max} (μg/ml)	$AUC_{0\rightarrow\infty}$ (μg·h/ml)	$MRT_{0\rightarrow\infty}$ (h)	Cl (ml/h/g)	V_{ss} (ml/g)
2% Pyro liposomes	21.9	250.1	4837	29.3	0.002	0.06
0% Pyro liposomes	16.9	275.0	5695	22.8	0.002	0.04
10%HPPH liposomes	1.6	224.2	581	2.1	0.02	0.04

MRT; median residence time. AUC; the area under the product of c·t plotted against t from time 0 to infinity. Cl, clearance. V_{SS}, volume of distribution at steady state.